THE JOURNAL OF BIOLOGICAL CHEMISTRY
Vol. 279, No. 39, Issue of September 24, pp. 40328–40336, 2004

Printed in U.S.A.

Inhibition of Mitochondrial Na^+-Ca^{2+} Exchange Restores Agonist-induced ATP Production and Ca^{2+} Handling in Human Complex I Deficiency*

Received for publication, July 16, 2004
Published, JBC Papers in Press, July 21, 2004, DOI 10.1074/jbc.M408068200

Henk-Jan Visch‡§¶‖, Guy A. Rutter‡‡, Werner J. H. Koopman‡¶§§, Jan B. Koenderink‡¶, Sjoerd Verkaart‡§¶‖, Theun de Groot‡¶, Aniko Varadi**, Kathryn J. Mitchell**, Lambert P. van den Heuvel§‖, Jan A. M. Smeitink§‖¶¶, and Peter H. G. M. Willems‡¶§§**

*From the Departments of ‡Biochemistry and §Pediatrics and the §§Microscopical Imaging Center, Nijmegen Centers of ¶Molecular Life Sciences and ‖Mitochondrial Disorders, University Medical Center Nijmegen, NL-6500 HB Nijmegen, The Netherlands and the **Henry Wellcome Signalling Laboratories and Department of Biochemistry, University of Bristol, BS8 1TD Bristol, United Kingdom*

Human mitochondrial complex I (NADH:ubiquinone oxidoreductase) of the oxidative phosphorylation system is a multiprotein assembly comprising both nuclear and mitochondrially encoded subunits. Deficiency of this complex is associated with numerous clinical syndromes ranging from highly progressive, often early lethal encephalopathies, of which Leigh disease is the most frequent, to neurodegenerative disorders in adult life, including Leber's hereditary optic neuropathy and Parkinson disease. We show here that the cytosolic Ca^{2+} signal in response to hormonal stimulation with bradykinin was impaired in skin fibroblasts from children between the ages of 0 and 5 years with an isolated complex I deficiency caused by mutations in nuclear encoded structural subunits of the complex. Inhibition of mitochondrial Na^+-Ca^{2+} exchange by the benzothiazepine CGP37157 completely restored the aberrant cytosolic Ca^{2+} signal. This effect of the inhibitor was paralleled by complete restoration of the bradykinin-induced increases in mitochondrial Ca^{2+} concentration and ensuing ATP production. Thus, impaired mitochondrial Ca^{2+} accumulation during agonist stimulation is a major consequence of human complex I deficiency, a finding that may provide the basis for the development of new therapeutic approaches to this disorder.

Human mitochondrial complex I (NADH:ubiquinone oxidoreductase) is the largest multisubunit assembly of the oxidative phosphorylation (OXPHOS)[1] system, comprising 39 nuclear encoded and seven mitochondrially encoded subunits. Malfunction of this complex is associated with a wide variety of clinical syndromes ranging from often early lethal disorders, of which Leigh disease, a progressive encephalopathy, is the most frequent, to neurodegenerative disorders in adulthood, including Leber's hereditary optic neuropathy and Parkinson disease. In recent years, all human nuclear structural complex I genes have been characterized, which allowed us to elucidate the genetic defect in 40% of a cohort of complex I-deficient patients in which the enzyme defect was present in at least skeletal muscle and cultured skin fibroblasts (1–7). To enhance our understanding of the pathophysiological consequences of these diseases, with the final aim of developing new treatment strategies to stabilize or even cure these conditions, we study genetically characterized human complex I-deficient fibroblast cell lines as a model for OXPHOS system disease, knowing that these cells are glycolytic (8). Several hypotheses concerning the pathophysiology of OXPHOS diseases have been investigated of which the most consistent are (*a*) increased production of reactive oxygen species (9), (*b*) decreased potential across the mitochondrial inner membrane (10), (*c*) decreased intracellular ATP levels (11–13), and (*d*) altered Ca^{2+} homeostasis (10, 12). In agreement with the reactive oxygen species hypothesis (*a*), we found that metallothioneins were up-regulated in all of the genetically characterized complex I-deficient cell lines (14). Pilot experiments with these cell lines furthermore revealed that human complex I deficiency was associated with altered cytosolic Ca^{2+} homeostasis. This encouraged us to undertake a detailed analysis of ATP production and calcium handling in a skin fibroblast cell line derived from a Leigh disease patient harboring a homozygous missense mutation (G364A) in the nuclear *NDUFS7* gene (4). Expression of this specific mutation in *Yarrowia lipolytica* confirmed the deleterious effect on complex I enzyme activity (15). The human NDUFS7 protein is one of the most conserved subunits of complex I and plays a central role in the interaction with the electron acceptor ubiquinone and in the proton-translocating mechanism (16, 17). Here we show that altered cytosolic Ca^{2+} handling in complex I-deficient cells with a mutation in the

* This work was supported by 6th Framework Programma Integrated Project Grant LSHM-CT-2004-503116 from the European Community and a Van Walree Fund grant from the Royal Netherlands Academy of Arts and Sciences. The costs of publication of this article were defrayed in part by the payment of page charges. This article must therefore be hereby marked "*advertisement*" in accordance with 18 U.S.C. Section 1734 solely to indicate this fact.

‡‡ Supported by Wellcome Trust Research Leave Fellowship and Programme Grant 067081/Z/02/Z, the Human Frontiers Science Program, the Medical Research Council (United Kingdom), and Diabetes UK.

¶¶ To whom correspondence should be addressed: Nijmegen Center for Mitochondrial Disorders, Dept. of Pediatrics, University Medical Center Nijmegen, P. O. Box 9101, NL-6500 HB Nijmegen, The Netherlands. Tel.: 31-243614430; Fax: 31-243616428; E-mail: j.smeitink@cukz.umcn.nl.

[1] The abbreviations used are: OXPHOS, oxidative phosphorylation; NDUFS7, NADH dehydrogenase ubiquinone flavoprotein S7 subunit; BHQ, 2,5-di-*tert*-butyl-benzohydroquinone; FCCP, carbonyl cyanide *p*-trifluoromethoxyphenylhydrazone; MELAS, myopathy, encephalopathy, lactic acidosis, stroke-like episodes; MERRF, myoclonic epilepsy with ragged red fibers; $[Ca^{2+}]_C$, $[Ca^{2+}]_{ER}$, and $[Ca^{2+}]_M$, cytosolic, endoplasmic reticular, and mitochondrial free Ca^{2+} concentrations; $[ATP]_C$ and $[ATP]_M$, cytosolic and mitochondrial ATP concentrations; ER, endoplasmic reticulum; $InsP_3$, inositol 1,4,5-trisphosphate; CMV, cytomegalovirus; KRB, Krebs-Ringer bicarbonate medium; SERCA, sarco-(endo)plasmic reticulum Ca^{2+}-ATPase.

NDUFS7 gene is associated with reduced mitochondrial Ca^{2+} accumulation and consequent ATP synthesis. An acute rescue of the defects was achieved following treatment with CGP37157, a benzothiazepine specifically inhibiting mitochondrial Na^+-Ca^{2+} exchange.

EXPERIMENTAL PROCEDURES

Chemicals—Culture material was obtained from Invitrogen, and fluorescent dyes were from Molecular Probes Inc. (Leiden, The Netherlands). CGP37157 was purchased from Tocris Cookson Ltd. (Avonmouth, Bristol, UK), and all other reagents were from Sigma.

Patient Fibroblasts—Fibroblasts were derived from skin biopsies of four healthy subjects and eight patients in the age range of 0–5 years in whom an isolated enzymatic complex I deficiency had been confirmed in both muscle tissue and cultured fibroblasts. The patient cells carried mutations the *NDUFS1*,[2] *NDUFS2* (1), *NDUFS4* (2, 3), *NDUFS7* (4), or *NDUFV1* (6) gene. Skin fibroblasts were cultured in M199 medium containing 5 mg/liter Tween 20 and supplemented with 10% fetal calf serum, 100 IU/ml penicillin, and 100 IU/ml streptomycin.

Fluorescence Imaging of Cytosolic Ca^{2+}—Fibroblasts were seeded on 22-mm glass coverslips, grown to subconfluence for 24 h, and loaded with Fura-2 in the presence of 3 μM Fura-2/AM for 25 min at 37 °C. After removal of excess dye, the coverslip was mounted in a thermostatic (37 °C) perfusion chamber placed on the stage of an inverted microscope (Nikon Diaphot). Dynamic video imaging was carried out using the MagiCal hardware and Tardis software as described previously (18). Cells were perfused with Hepes-Tris medium (132 mM NaCl, 4.2 mM KCl, 1 mM $CaCl_2$, 1 mM $MgCl_2$, 5.5 mM D-glucose, and 10 mM Hepes, pH 7.4), supplemented with an amino acid mixture according to Eagle, and challenged with 1 μM bradykinin to increase the cytosolic free Ca^{2+} concentration ($[Ca^{2+}]_C$). The Fura-2 fluorescence emission ratio at 492 nm was monitored as a measure of $[Ca^{2+}]_C$ after alternating excitation at 340 and 380 nm. The kinetics with which the fluorescence emission ratio decreased was fitted to a monoexponential equation, $R(t) = R(t = 0)\cdot e^{-\lambda\cdot t} + R(P)$, where λ is the decay constant (in s) and $R(P)$ is the poststimulatory level to which R declines. From λ the half-time ($t_{½}$) was calculated using the equation $t_{½}(s) = -\ln(0.5)\cdot\lambda$.

Luminescence Monitoring of Cytosolic ATP, Endoplasmic Reticular Ca^{2+}, and Mitochondrial Ca^{2+} and ATP—Because primary human skin fibroblasts are refractory to most conventional transfection protocols, we used an adenoviral system to express mitochondrially targeted aequorin (*AdCMVmAq*), mitochondrially targeted luciferase (*AdCMVmLuc*), and cytosolic luciferase (*AdCMVcLuc*) (19, 20), whereas a baculoviral system was used to express endoplasmic reticulum-targeted aequorin (*BvCMVeAq*). The latter system, which is normally used for protein production in *Spodoptera frugiperda* 9 insect cells, was made suitable for protein expression in mammalian cells by first removing the herpes simplex virus thymidine kinase polyadenylation signal from the pFastBacTMDual vector (Invitrogen) using AccI and XhoI, by next, after blunting and ligation, removing both the p10 and polyhedron promoter with SmaI and XbaI, and by replacing it with the coding region of a cytomegalovirus (CMV) promoter digested from the pcDNA1 vector (Invitrogen) using NruI and XbaI. Finally, the cDNA of ER-targeted aequorin was digested from the erAEQmut/pcDNA1 vector described by Montero *et al.* (21) with KpnI and NsiI and ligated behind the CMV promoter in the KpnI and PstI restriction sites of the modified baculovirus vector. Approximately 25,000 cells were spotted on a 13-mm coverslip, and after 24 h cells were infected with the appropriate virus and cultured for another 48 h. In case of baculoviral infection, the culture medium contained 1.75 mM sodium butyrate for proper expression of the photoprotein.

Luciferase luminescence was monitored continuously using a photomultiplier tube (Thorn EMI Electron tubes, Ruislip, Middlesex, UK) (19). Cells were perfused (2 $ml\cdot min^{-1}$) with modified Krebs-Ringer bicarbonate medium (KRB; 140 mM NaCl, 3.5 mM KCl, 0.5 mM NaH_2PO_4, 0.5 mM $MgSO_4$, 10 mM Hepes, 2 mM $NaHCO_3$, 1 mM $CaCl_2$, 5.5 mM D-glucose, pH 7.4) containing 5 μM beetle luciferin (Promega, Madison, WI) at 37 °C. Emitted light was collected with a photon-counting board using the supplier's software (Thorn EMI) (22). Light output was recorded at 1-s intervals after which the traces were smoothed off-line by using a 5-point moving average (Origin Pro 6.1, OriginLab Corporation, Northampton, MA). Typically, light output from a coverslip of virally infected fibroblasts was 1,000–25,000 $counts\cdot s^{-1}$ *versus* a background of 10 $counts\cdot s^{-1}$. The same system was used to monitor aequorin luminescence. Mitochondrial aequorin was reconstituted with 5 μM coelenterazine (Molecular Probes) in KRB for 1 h at 37 °C. Light output was recorded at 1-s intervals, and at the end of each experiment the signal was calibrated by lysing the cells with 100 μM digitonin and 10 mM $CaCl_2$ to determine the total photoprotein content. Aequorin photon emission was converted off-line into $[Ca^{2+}]$ values using a computer algorithm based on the Ca^{2+} response curve of wild-type aequorin (23). For measurements of endoplasmic reticulum aequorin, we first reduced the Ca^{2+} content of this organelle by incubating the cells with a reversible inhibitor of the ER Ca^{2+}-ATPase, BHQ (10 μM), in Ca^{2+}-free KRB (no $CaCl_2$ added and 0.5 mM EGTA present) for 10 min. After washing, endoplasmic reticulum aequorin was reconstituted with 5 μM coelenterazine n (Molecular Probes) in Ca^{2+}-free KRB containing 10 μM BHQ for 1.5 h at room temperature. Next, the glass coverslip was placed in the luminometer, and cells were initially perfused with Ca^{2+}-free KRB for 5 min at 37 °C to remove BHQ.

To determine the sarco(endo)plasmic reticulum Ca^{2+}-ATPase (SERCA)-mediated Ca^{2+} uptake activity, cells were perfused with a Ca^{2+}-free intracellular medium (10 mM Hepes, 120 mM KCl, 5 mM NaCl, 2.5 mM $MgCl_2$, 2 mM EGTA, 2.5 mM ATP, pH 7.05) containing 20 μg/ml saponin for 2 min at 37 °C to selectively permeabilize the plasma membrane (24). SERCA-mediated Ca^{2+} uptake into the ER was started by perfusing with intracellular medium containing 0.55 mM $CaCl_2$ (free Ca^{2+} concentration of 0.1 μM). The luminescence data were calibrated as described previously by Alvarez and Montero (25).

Fluorescence Imaging of Mitochondrial Membrane Potential ($\Delta\Psi_M$)—Fibroblasts were loaded with 0.5 μM JC-1 for 10 min. Next, coverslips (22 mm) were mounted in a perfusion chamber and placed on the stage of an inverted microscope (Axiovert 200 M, Carl Zeiss, Jena, Germany) equipped with a ×40, 1.3 NA F Fluar objective. Cells were perfused with KRB. JC-1 was excited at 488 nm using a monochromator (Polychrome IV, TILL Photonics, Gräfelfing, Germany). Fluorescence light was directed by a 505DRLPXR dichroic mirror (Omega Optical Inc., Brattleboro, VT) through either a 535AF26 (JC-1 monomers, green emission) or a 565ALP emission filter (JC-1 aggregates, red emission) (Omega) onto a CoolSNAP HQ monochrome CCD camera (Roper Scientific, Vianen, The Netherlands). All hardware was controlled with Metafluor 6.0 software (Universal Imaging Corporation, Downingtown, PA) running under Windows XP Professional on a personal computer equipped with 1-gigabyte random access memory (RAM). Images were digitalized, and the amount of J-aggregates/cell was automatically counted using Image Pro Plus 4.1 software (Media Cybernetics, Silver Spring, MD).

Determination of ATP Levels in Cell Homogenates—Pellets containing ~300,000 cells were immediately frozen in liquid nitrogen and subsequently resuspended in 1 ml of phosphate-buffered saline on ice. For determination of the total ATP content, a commercial kit was used based on luciferase (Roche Applied Science). Bioluminescence signals were measured with a Berthold MicroLumat Plus LB 96-V luminometer and expressed per mg of protein as determined using the Bio-Rad protein assay.

Data Analysis—Numerical values were visualized using Origin Pro 6.1 (OriginLab Corporation), and values from multiple experiments were expressed as average ± S.E. Statistical significances were assessed by Student's *t* test.

RESULTS

Impaired Cytosolic Ca^{2+} Handling in Complex I-deficient Human Fibroblasts—The present study was aimed at establishing the consequences of complex I deficiency on intracellular Ca^{2+} homeostasis in the context of the genetic background of the patient. Skin fibroblasts from four control individuals and eight patients with isolated enzymatic complex I deficiency caused by nuclear DNA mutations were loaded with the fluorescent Ca^{2+} indicator Fura-2 for monitoring of the bradykinin-induced changes in $[Ca^{2+}]_C$ in individual cells using digital imaging microscopy. An increase in $[Ca^{2+}]_C$ is reported by an increase in the ratio of the fluorescence emission intensities at excitation wavelengths of 340 and 380 nm.

Control fibroblasts displayed resting emission ratios of 0.48 ± 0.02 (n = 24), 0.48 ± 0.02 (n = 31), 0.54 ± 0.03 (n = 30), and 0.52 ± 0.02 (n = 29) that were not significantly different between the four individuals. Immediately after stimulation with bradykinin (1 μM) the cells displayed a sharp rise in $[Ca^{2+}]_C$ (see also Fig. 3*D*). Maximum increases in the emission

[2] J. A. M. Smeitink and L. P. van den Heuvel, unpublished data.

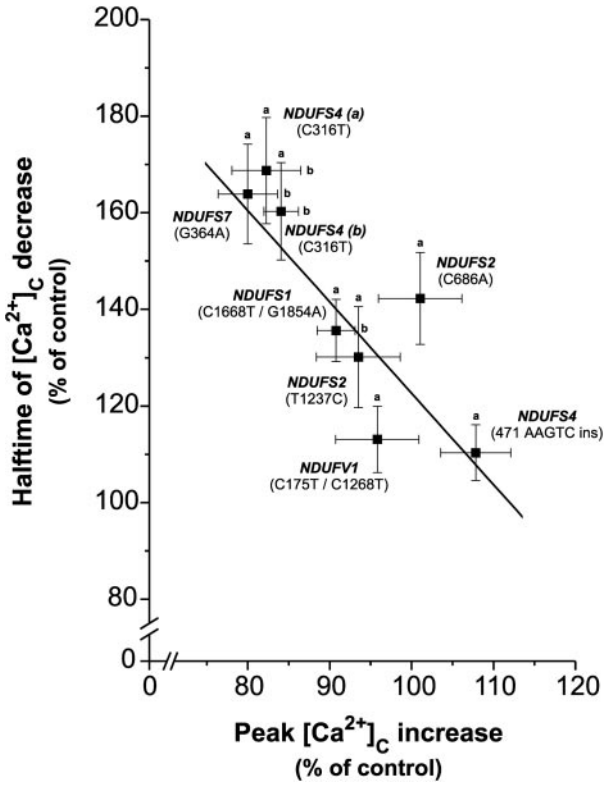

FIG. 1. **Impaired cytosolic Ca^{2+} handling in complex I-deficient fibroblasts.** Fura-2-loaded control and patient fibroblasts were challenged with 1 μM bradykinin, and the changes in $[Ca^{2+}]_C$ were monitored by digital imaging microscopy. For kinetic analysis, the fluorescence emission ratio was normalized to its prestimulatory value. The peak $[Ca^{2+}]_C$ increase (maximal increase in fluorescence emission ratio) and cytosolic Ca^{2+} removal rate (half-time of the decrease in fluorescence emission ratio) in control fibroblasts were set at 100%, to which all patient values were related. A linear fit, during which the S.E. of each *data point* was used as a weight (weight = $1/(S.E.)^2$), was performed to determine the correlation between both parameters. *a*, significantly different from the Ca^{2+} removal rate in control fibroblasts; *b*, significantly different from the peak $[Ca^{2+}]_C$ increase in control fibroblasts. Cell numbers and *p* values are given in the text.

ratio were 4.47 ± 0.15 (n = 24), 4.71 ± 0.19 (n = 31), 4.89 ± 0.19 (n = 30), and 4.74 ± 0.15 (n = 29) × base line and did not statistically differ. The amplitude of the $[Ca^{2+}]_C$ rise was independent of extracellular Ca^{2+}, demonstrating that Ca^{2+} ions entered the cytosolic compartment from the endoplasmic reticular Ca^{2+} store. After having reached its maximum, $[Ca^{2+}]_C$ more gradually declined again to prestimulatory levels. The decrease in fluorescence emission ratio was fitted monoexponentially, and half-times ($t_{½}$) were 12.6 ± 0.5 s (n = 24), 13.4 ± 0.5 s (n = 31), 13.4 ± 0.5 s (n = 30), and 14.1 ± 0.6 s (n = 29), suggesting the involvement of one major Ca^{2+} removal process. The $t_{½}$ values did not significantly differ between the four healthy individuals. On average, control fibroblasts (n = 114) displayed an emission ratio of 0.50 ± 0.01 at rest that increased to 4.71 ± 0.09 × base line following stimulation with bradykinin and subsequently decreased with a $t_{½}$ of 13.4 ± 0.3 s.

Patient and control fibroblasts did not differ with respect to the resting $[Ca^{2+}]_C$ (see also Fig. 3*D*). However, the bradykinin-induced peak increase in $[Ca^{2+}]_C$ was significantly decreased in four patients, whereas the rate of cytosolic Ca^{2+} removal was significantly, but to a variable degree, slowed down in all patients as indicated by an increase in half-time (Fig. 1). Fibroblasts with a mutation in either the *NDUFS4* (Fig. 1, C316T; n = 23 and n = 18 for patients *a* and *b*, respectively) or *NDUFS7* (G364A; n = 21) gene displayed both a marked reduction in peak $[Ca^{2+}]_C$ (~20%; $p < 0.001$) and a large increase in $t_{½}$ (1.6-fold; $p < 0.001$). The *NDUFS1* mutation (C1668T/G1854A; n = 16) showed a moderate reduction in peak height (~10%; $p < 0.05$) and a moderate increase in $t_{½}$ (1.3-fold; $p < 0.001$), whereas the two *NDUFS2* mutations, C686A (n = 20) and T1237C (n = 22), displayed only a moderate increase in $t_{½}$ (1.4- and 1.3-fold, respectively; $p < 0.001$). Finally, the *NDUFS4* (471 AAGTC insertion; n = 31); and *NDUFV1* (C175T/C1268T; n = 20) mutations displayed a small increase in $t_{½}$ (1.1-fold; $p < 0.05$) and no change in peak height.

A significant ($p < 0.01$) correlation was observed between peak height and Ca^{2+} removal rate, indicating a common cause for their reduction in human complex I deficiency (Fig. 1). Because of the marked effects observed with fibroblasts carrying a G364A mutation in the *NDUFS7* gene, we used these cells in a series of experiments conducted to gain insight into the mechanism(s) underlying the changes in cytosolic Ca^{2+} handling in human complex I deficiency.

Reduced Filling State of the Endoplasmic Reticular Ca^{2+} Store in Unstimulated Complex I-deficient Fibroblasts—The bradykinin-induced $[Ca^{2+}]_C$ transients in fibroblasts are likely to be shaped mainly by the relative rates of (i) Ca^{2+} release from the ER into the cytoplasm, (ii) Ca^{2+} uptake and subsequent release by mitochondria, and (iii) cytosolic Ca^{2+} removal via SERCAs and plasma membrane Ca^{2+}-ATPases. To investigate whether the ER Ca^{2+} content is altered in resting patient fibroblasts with a G364A mutation in the *NDUFS7* gene, cells were loaded with Fura-2 and subsequently treated with the Ca^{2+} ionophore ionomycin. Measurements were performed in the absence of extracellular Ca^{2+} to prevent capacitative Ca^{2+} entry in response to Ca^{2+} store depletion. Ionomycin (1 μM) transiently increased $[Ca^{2+}]_C$ in both control and patient fibroblasts (Fig. 2*A*). The area under the peak was ~20% lower in patient fibroblasts (Fig. 2*A*, 79 ± 2%, n = 19; $p < 0.001$), indicating that the Ca^{2+} content of the ER is significantly reduced in complex I deficiency. Reduction of the ER Ca^{2+} content may point to a decreased rate of Ca^{2+} uptake or an increased rate of Ca^{2+} leakage.

To determine possible differences in SERCA number and/or transport properties, fibroblasts expressing ER-targeted aequorin were first permeabilized with saponin in a Ca^{2+}-free intracellular medium containing 2.5 mM ATP. Next, SERCA-mediated Ca^{2+} uptake was started by increasing the free $[Ca^{2+}]$ of the perfusion medium to 0.1 μM, which equals the cytosolic free $[Ca^{2+}]$ in unstimulated cells. Both control and patient fibroblasts showed a rapid increase in $[Ca^{2+}]_{ER}$ (Fig. 2*B*). The maximal rate of $[Ca^{2+}]_{ER}$ increase was not different between control (13 ± 1 $\mu M \cdot s^{-1}$, n = 6) and patient (12 ± 1 $\mu M \cdot s^{-1}$, n = 6) fibroblasts. Similarly, the peak $[Ca^{2+}]_{ER}$, which was reached after ~60 s, was not different between control (442 ± 22 μM, n = 6) and patient fibroblasts (449 ± 17 μM, n = 6). These findings demonstrate that under conditions in which ATP is not rate-limiting, both the SERCA activity and the physical size of the ER Ca^{2+} store are the same for control and patient fibroblasts.

To address the possibility that Ca^{2+} leakage from the ER is increased in patient fibroblasts, cells were loaded with Fura-2 and subsequently treated with the SERCA inhibitor BHQ in the absence of extracellular Ca^{2+}. Both in control and patient fibroblasts, BHQ (10 μM) evoked an immediate increase in $[Ca^{2+}]_C$ (Fig. 2*C*). The maximal rate of $[Ca^{2+}]_C$ increase was not significantly different between control (0.016 ± 0.001 arbitrary unit$\cdot s^{-1}$, n = 13) and patient (0.016 ± 0.001 arbitrary unit$\cdot s^{-1}$, n = 16) fibroblasts. In contrast, the peak $[Ca^{2+}]_C$ was significantly ($p < 0.001$) lower in patient (1.42 ± 0.01 × base line) as compared with control fibroblasts (1.58 ± 0.01 × base line). The latter finding is compatible with a decreased ER

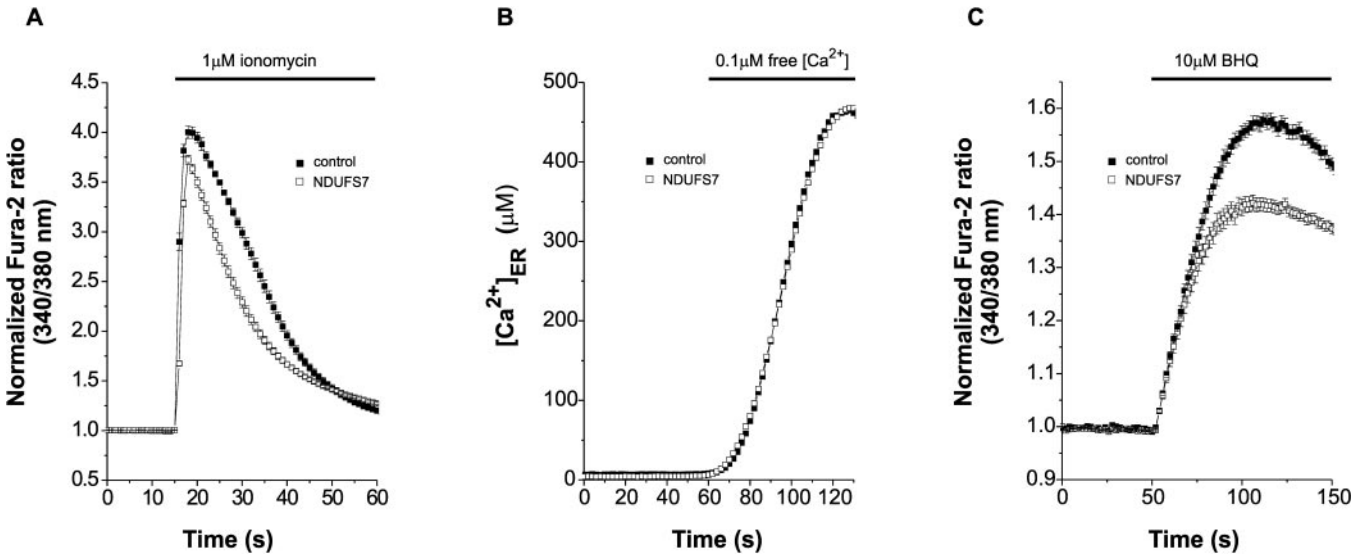

FIG. 2. **Reduced filling state of the internal Ca^{2+} store in complex I-deficient fibroblasts.** Fura-2-loaded control and patient fibroblasts were treated with 1 μM ionomycin (*A*) or 10 μM BHQ (*C*), and changes in $[Ca^{2+}]_C$ were monitored by digital imaging microscopy. Measurements were performed in the absence of external Ca^{2+} (no $CaCl_2$ added and 0.5 mM EGTA present). In each experiment, the fluorescence emission ratio was normalized to its prestimulatory value. Depicted are averaged traces of the number of cells given in the text. Control and patient fibroblasts expressing ER-targeted aequorin were permeabilized by saponin treatment to determine the rate of SERCA-mediated Ca^{2+} uptake and the Ca^{2+} uptake capacity of the internal Ca^{2+} store (*B*). Permeabilized fibroblasts were perfused with a Ca^{2+}-free intracellular medium (no $CaCl_2$ added and 2.0 mM EGTA present) containing 2.5 mM ATP. At the indicated time, SERCA-mediated Ca^{2+} uptake into the ER was started by increasing the free Ca^{2+} concentration in the perfusion medium to 0.1 μM. Depicted are typical traces of control and patient coverslips. Details on the quantitative analysis of the signals are given in the text.

Ca^{2+} content in resting complex I-deficient fibroblasts. Finally, measurement of the total ATP content in whole cell lysates using a luciferase-based assay revealed a small (5%) but statistically insignificant decrease in patient fibroblasts ($p = 0.08$; $n = 4$ for both control and patient fibroblasts).

Decreased Mitochondrial Ca^{2+} Accumulation in Bradykinin-stimulated Complex I-deficient Fibroblasts—It has been shown previously that agonist-induced increases in $[Ca^{2+}]_C$ lead to parallel increases in the total (26) and free (27, 28) concentration of Ca^{2+} in mitochondria ($[Ca^{2+}]_M$). To investigate whether mitochondrial Ca^{2+} accumulation is altered in complex I deficiency, patient fibroblasts were infected with adenoviruses expressing mitochondrially targeted aequorin. The cells (~25,000) were challenged with 1 μM bradykinin, and the changes in $[Ca^{2+}]_M$ were monitored. The peak increase in $[Ca^{2+}]_M$, which was observed at ~12 s after the onset of stimulation, was significantly ($p < 0.05$) decreased from 4.23 ± 0.21 μM ($n = 6$) in control cells to 3.36 ± 0.20 μM ($n = 6$) in patient cells (Fig. 3*A*). The $t_{½}$ values of the $[Ca^{2+}]_M$ decrease did not differ between control (6.0 ± 0.5 s) and patient (6.5 ± 0.3 s) fibroblasts.

Pretreatment of the cells with the protonophore FCCP (1 μM, 2 min) completely abolished the bradykinin-induced increase in $[Ca^{2+}]_M$. In contrast, the drug inhibited the bradykinin-induced peak increase in $[Ca^{2+}]_C$ only by 25% (see also Fig. 4*A*). This demonstrates that aequorin was exclusively present in the mitochondrial compartment.

Reduced Mitochondrial Membrane Potential in Complex I-deficient Fibroblasts—Studies using suspensions of isolated mitochondria have suggested that mitochondrial Ca^{2+} uptake is mediated by an electrogenic "low affinity" uniporter ($K_{0.5}$ = 5–10 μM) driven by the large electrical gradient ($\Delta\Psi_M \approx -160$ mV) created by the respiratory chain (29, 30). However, by patch-clamping vesicles of the inner mitochondrial membrane, Clapham and co-workers (31) were able to demonstrate recently that the mitochondrial Ca^{2+} uptake system is, in fact, a highly selective Ca^{2+} channel with a half-activation constant of 19 mM. It has been demonstrated that a decrease in respiratory activity results not only in a reduction in $\Delta\Psi_M$ (10) but also in a decrease in agonist-stimulated mitochondrial Ca^{2+} uptake (12). To assess whether the $\Delta\Psi_M$ is decreased in complex I-deficient cells, patient fibroblasts were loaded with the fluorescent dye JC-1, which accumulates within the mitochondrial matrix as a function of $\Delta\Psi_M$ (32). At high concentrations this dye forms J-aggregates with a red fluorescence emission signal. Counting of the number of red objects/cell revealed a significant ($p < 0.01$) difference between patient (89 ± 3, $n = 42$) and control (104 ± 3, $n = 39$) fibroblasts. Pretreatment with 1 μM FCCP for 2 min reduced the amount of J-aggregates to 4 ± 1 ($n = 11$), demonstrating their dependence on $\Delta\Psi_M$.

Reduced Mitochondrial ATP Production in Bradykinin-stimulated Complex I-deficient Fibroblasts—Agonist-induced increases in $[Ca^{2+}]_M$ have been shown previously to cause activation of intramitochondrial dehydrogenases (33, 34) and consequent increases in NAD(P)H and $FADH_2$ (35, 36). This in turn stimulates respiratory chain activity and mitochondrial ATP synthesis (12, 37). To investigate whether mitochondrial ATP production is altered in complex I deficiency, patient fibroblasts were infected with adenoviruses expressing mitochondrially targeted or cytosolic firefly luciferase. Bradykinin evoked a gradual increase in both $[ATP]_M$ (Fig. 3*B*) and $[ATP]_C$ (Fig. 3*C*) that lasted ~40 s and started ~20 s after the onset of stimulation and ~8 s after $[Ca^{2+}]_M$ had reached its maximum. Subsequently, the ATP concentrations more gradually decreased again to prestimulatory levels. Pretreatment of cells expressing mitochondrially targeted luciferase with the mitochondrial ATP synthase inhibitor oligomycin (10 μM, 10 min) resulted in complete inhibition of the bradykinin-induced increase in luminescence (data not shown). With respect to $[ATP]_M$, both rising speed and peak value were significantly ($p < 0.01$) decreased in patient fibroblasts (rising speeds of 0.33 ± 0.05%·s^{-1} and 0.14 ± 0.02%·s^{-1} and peak values of 109.3 ± 0.8% and 104.5 ± 1.0% for control ($n = 7$) and patient ($n = 5$) cells, respectively). Regarding the bradykinin-induced increase in $[ATP]_C$, however, the rising speed and peak value did not significantly

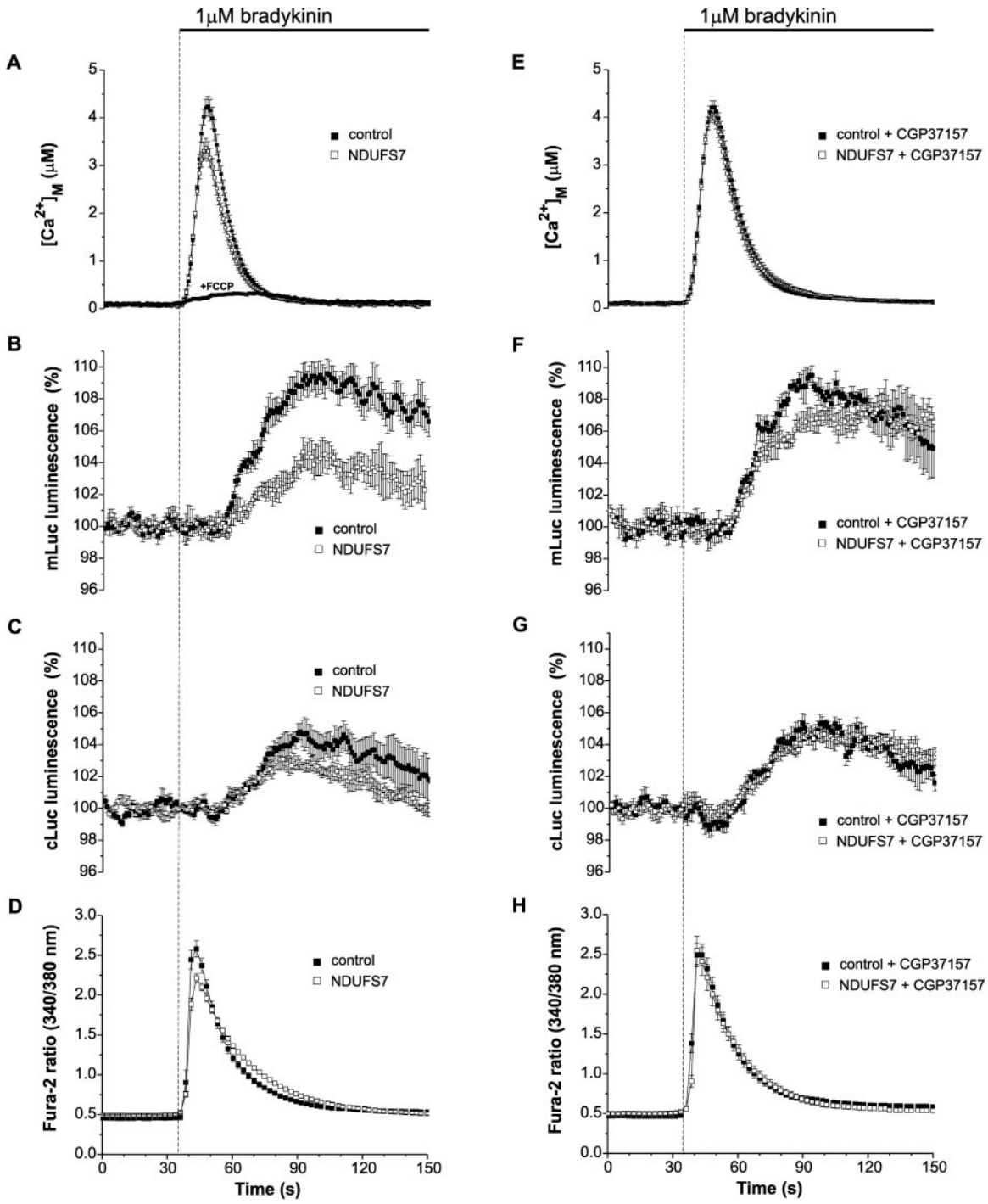

FIG. 3. **Restoration of impaired Ca^{2+} and ATP handling in complex I-deficient fibroblasts by CGP37157.** Cells were incubated in the absence (*A–D*) or presence (*E–H*) of CGP37157 (1 μM) for 2 min and stimulated with bradykinin (1 μM) at the indicated time. Bradykinin-induced changes in cytosolic and mitochondrial $[Ca^{2+}]$ and [ATP] were monitored by either luminometry (*A–C* and *E–G*) or fluorometry (*D* and *H*). In each ATP measurement (*B*, *C*, *F*, and *G*), the luminescence signal was expressed relative to its prestimulatory value. Depicted are averaged traces of the number of coverslips (*A–C* and *E–G*) and cells (*D* and *H*) given in the text. Details on the quantitative analysis of the signals are given in the text. *cLuc*, cytosolic luciferase; *mLuc*, mitochondrially targeted luciferase.

differ between control and patient fibroblasts (rising speeds of 0.18 ± 0.03%·s^{-1} and 0.11 ± 0.01%·s^{-1} and peak values of 104.7 ± 0.8% and 103.0 ± 0.6% for control (n = 3) and patient (n = 3) cells, respectively).

Fig. 3*D* compares the bradykinin-induced changes in $[Ca^{2+}]_C$ between Fura-2-loaded control and patient fibroblasts. In both cases, the peak increase in $[Ca^{2+}]_C$ was observed ~8 s after the onset of stimulation. The amplitude of the $[Ca^{2+}]_C$ rise was significantly ($p < 0.01$) decreased in patient fibroblasts (maximum emission ratios of 5.7 ± 0.2 and 4.6 ± 0.1 × base line for control (n = 17) and patient (n = 30) cells, respectively). The $t_{½}$ of the subsequent $[Ca^{2+}]_C$ decline was significantly ($p < 0.001$) increased in patient fibroblasts ($t_{½}$ values of 11.8 ± 0.6 s and 18.2 ± 1.0 s for control (n = 17) and patient (n = 30) cells, respectively).

Restoration of Impaired Ca^{2+} and ATP Homeostasis by CGP37157 in Human Complex I-deficient Fibroblasts—It has been demonstrated that cells of a cybrid cell line of ρ^0-osteosarcoma cells and enucleated cytoplasts from a patient with the $tRNA^{Lys}$ mutation of myoclonic epilepsy with ragged red fibers

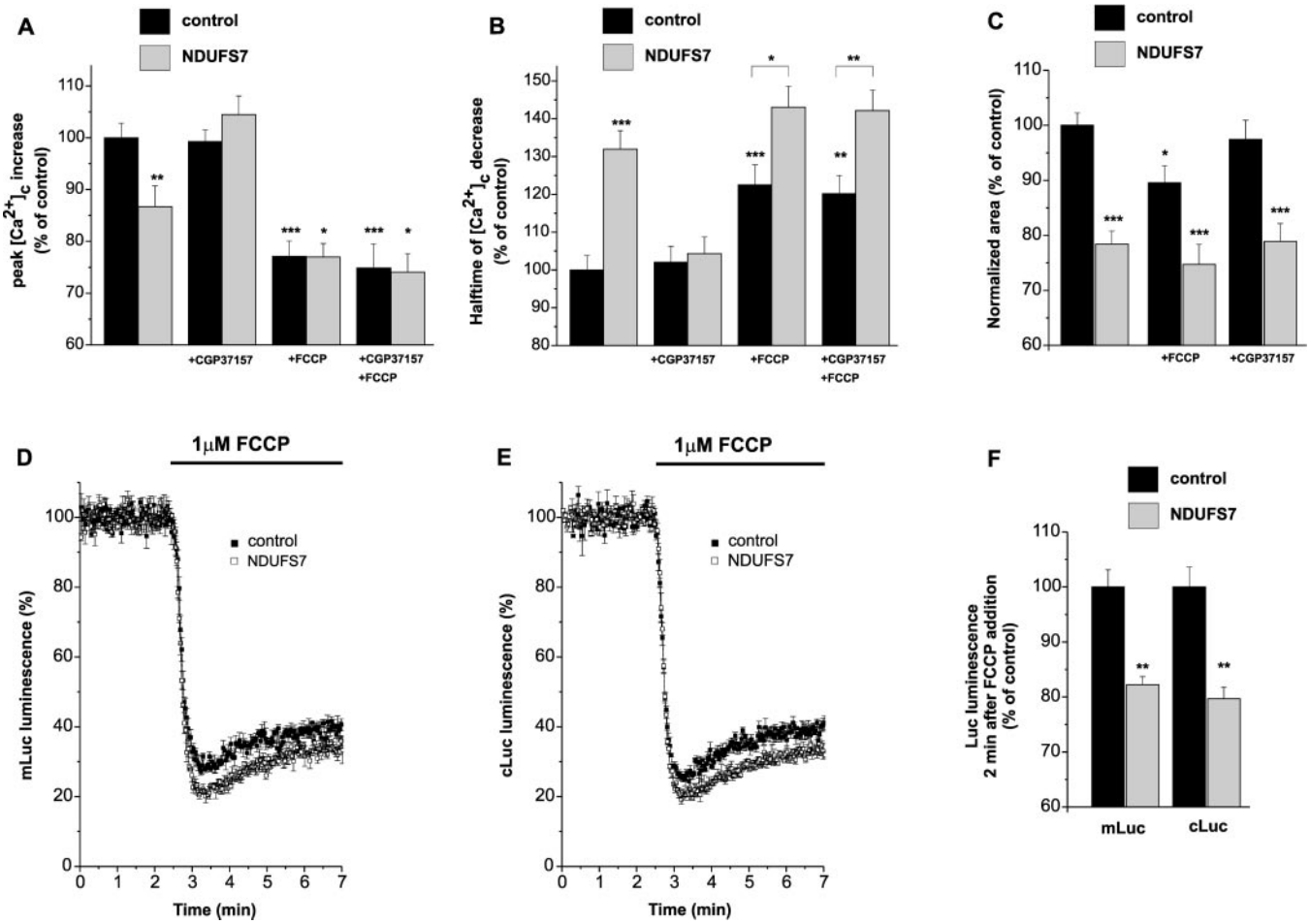

FIG. 4. **Restorative effect of CGP37157 depends on $\Delta\Psi_M$.** Fura-2-loaded cells were stimulated with bradykinin (1 μM; *A* and *B*) or treated with ionomycin (1 μM; *C*) in the absence and presence of CGP37157 (1 μM) and/or FCCP (1 μM) added 2 min prior to stimulation. Measurements were performed in the absence of external Ca^{2+} (no $CaCl_2$ added and 0.5 mM EGTA present). Shown is the effect on the bradykinin-induced peak increase in $[Ca^{2+}]_C$ (*A*), the half-time of the cytosolic Ca^{2+} decrease (*B*), and the ER Ca^{2+} content in resting fibroblasts (*C*). The averaged value of untreated controls is set at 100%, to which all values are related. Fibroblasts expressing either mitochondrially targeted (*mLuc*; *D* and *F*) or cytosolic luciferase (*cLuc*; *E* and *F*) were treated with FCCP (1 μM) for the indicated period of time. The effect on the mitochondrial (*D*) and the cytosolic luminescence signal (*E*) is shown. In each measurement, the luminescence signal was expressed relative to its value before FCCP treatment. The mitochondrial and cytosolic luminescence level at 2 min after the onset of FCCP treatment is shown in *F*. The averaged value of FCCP-treated controls is set at 100%, to which the corresponding patient values are related. *, $p < 0.05$; **, $p < 0.01$; ***, $p < 0.001$.

(MERRF) display impaired mitochondrial, but not cytosolic, Ca^{2+} handling following agonist stimulation (12). The same study showed that mitochondrial Ca^{2+} handling and the ensuing stimulation of ATP production were largely restored with CGP37157, a specific inhibitor of mitochondrial Na^+-Ca^{2+} exchange (38). To investigate whether this drug exerts restorative effects in complex I-deficient fibroblasts, we pretreated control and patient cells with 1 μM CGP37157 for 2 min and monitored the bradykinin-induced changes in $[Ca^{2+}]_M$ (Fig. 3*E*), $[ATP]_M$ (Fig. 3*F*), $[ATP]_C$ (Fig. 3*G*), and $[Ca^{2+}]_C$ (Fig. 3*H*). The drug did not affect the bradykinin-induced increase in $[Ca^{2+}]_M$ in control fibroblasts but completely restored this parameter in patient cells (peak values of 4.21 ± 0.13 μM and 4.06 ± 0.13 μM for CGP37157-treated control ($n = 6$) and patient ($n = 6$) cells, respectively) (Fig. 3*E*). Moreover, the drug significantly ($p < 0.05$) increased the half-time of the $[Ca^{2+}]_M$ decrease in both control and patient cells to 7.8 ± 0.5 s and 8.5 ± 0.7 s for control ($n = 6$) and patient ($n = 6$) cells, respectively. CGP37157 did not alter the resting $[Ca^{2+}]_M$.

Next, we addressed the question of whether restoration of mitochondrial Ca^{2+} uptake resulted in enhanced activation of the OXPHOS system. In patient fibroblasts, CGP37157 increased both the rising speed and the peak value of the bradykinin-induced $[ATP]_M$ increase to control values (rising speed of 0.31 ± 0.04%·s^{-1} and peak value of 107.8 ± 0.6%, $n = 5$) (Fig. 3*F*). The drug did not affect these parameters in control cells (rising speed of 0.37 ± 0.03%·s^{-1} and peak value of 109.4 ± 0.6%, $n = 4$). The restoration of agonist-induced mitochondrial ATP production was accompanied by an increase in rising speed and peak value of the $[ATP]_C$ increase (rising speed of 0.17 ± 0.01%·s^{-1} and peak value of 104.8 ± 0.3%, $n = 4$) (Fig. 3*G*). The drug did not significantly alter these parameters in control cells (rising speed of 0.18 ± 0.01%·s^{-1} and peak value of 105.3 ± 0.4%, $n = 4$).

Finally, we investigated the effect of this drug on the bradykinin-induced $[Ca^{2+}]_C$ rise in Fura-2-loaded patient fibroblasts. CGP37157 completely restored both the bradykinin-induced peak increase in $[Ca^{2+}]_C$ and the $t_{½}$ of the subsequent $[Ca^{2+}]_C$ decrease to control values (maximum emission ratio of 5.4 ± 0.3 × base line and $t_{½}$ value of 12.2 ± 0.7 s, $n = 19$) (Fig. 3*H*). The drug did not alter these parameters in control fibroblasts (maximum ratio value of 5.6 ± 0.3 × base line and $t_{½}$ value of 11.5 ± 0.8 s, $n = 18$). The drug also did not alter the resting $[Ca^{2+}]_C$.

CGP37157-induced Restoration of Cytosolic Ca^{2+} Handling in Complex I-deficient Fibroblasts Depends on the Mitochondrial Membrane Potential—To investigate the possible involvement of extracellular Ca^{2+} influx in the mechanism of action of

CGP37157, Fura-2-loaded cells were stimulated in the absence of external Ca^{2+} (no Ca^{2+} added and 0.5 mM EGTA present). Also under these conditions patient fibroblasts displayed a decrease in bradykinin-induced peak $[Ca^{2+}]_C$ (Fig. 4*A*) and an increase in $t_{½}$ of the subsequent $[Ca^{2+}]_C$ decrease (Fig. 4*B*) that were fully restored by CGP37157. These findings demonstrate that both the defect and its restoration by CGP37157 are independent of external Ca^{2+}. CGP37157 did not change the area under the ionomycin-evoked $[Ca^{2+}]_C$ transient (97 ± 3% and 79 ± 3% for CGP37157-treated control ($n = 19$) and patient ($n = 29$) fibroblasts, respectively) (Fig. 4*C*). This indicates that the drug does not affect the filling state of the internal Ca^{2+} stores.

The importance of $\Delta\Psi_M$ for the restorative effect of CGP37157 was investigated using the protonophore FCCP. FCCP, when added at a concentration of 1 μM, caused the complete loss of mitochondrial rhodamine 123 staining within 1 min after its addition, demonstrating the rapid breakdown of the mitochondrial membrane potential (data not shown). Within the same time frame, FCCP caused a marked decrease in $[ATP]_M$ (Fig. 4*D*) and $[ATP]_C$ (Fig. 4*E*). The ATP level before drug treatment was set at 100%, demonstrating that in both the mitochondrial matrix and cytoplasm the FCCP-induced decrease in ATP was higher in patient fibroblasts. Similarly, at 2 min after the onset of drug treatment the ATP level in both mitochondrial matrix and cytoplasm was 20% ($p < 0.01$) lower in patient fibroblasts (Fig. 4*F*).

Regarding the effect of FCCP on $[Ca^{2+}]_{ER}$, only a small reduction was observed at 2 min after addition of the drug (Fig. 4*C*). In control cells this reduction was 11% ($n = 22$), whereas in patient cells this reduction was 5% ($n = 28$).

With respect to the bradykinin-induced $[Ca^{2+}]_C$ transient, pretreatment of control cells with 1 μM FCCP for 2 min significantly ($p < 0.001$) decreased the peak increase in $[Ca^{2+}]_C$ by ~25% (Fig. 4*A*). In addition, the drug significantly ($p < 0.001$) slowed down the rate of cytosolic Ca^{2+} removal (Fig. 4*B*). Notably, the peak increase in $[Ca^{2+}]_C$ was exactly the same in FCCP-treated control and patient fibroblasts, indicating that ~25% of the bradykinin-induced peak increase in $[Ca^{2+}]_C$ depends on an intact mitochondrial membrane potential. The observation that the peak $[Ca^{2+}]_C$ increase was decreased by ~15% in patient fibroblasts (Fig. 4*A*) is in agreement with the idea that the mitochondrial membrane potential is partly reduced in these cells. FCCP did not significantly alter the rate of cytosolic Ca^{2+} removal in patient fibroblasts (Fig. 4*B*). Of note, the rate of cytosolic Ca^{2+} removal was still significantly higher in FCCP-treated control cells as compared with FCCP-treated patient cells (Fig. 4*B*). This is in line with the finding that the FCCP-induced decrease in both $[ATP]_M$ and $[ATP]_C$ is less in control cells as compared with patient cells (Fig. 4, *D–F*). Importantly, the restorative effect of CGP37157 was completely abolished in FCCP-treated patient fibroblasts, indicating that an intact mitochondrial membrane potential is required for the drug to exert its effect (Fig. 4, *A* and *B*).

DISCUSSION

Human complex I (NADH:ubiquinone oxidoreductase) deficiency leads to a wide variety of clinical disease presentations, of which the underlying cell biological causes are poorly understood (7). Here we show that mitochondrial membrane potential and, as a consequence, agonist-induced mitochondrial Ca^{2+} uptake and ensuing stimulation of mitochondrial ATP production are impaired in skin fibroblasts from a patient with Leigh disease carrying a homozygous missense mutation (G364A) in the nuclear *NDUFS7* gene (4). We also show that the impairments in mitochondrial function are associated with a reduced filling state of the ER Ca^{2+} store, a decreased agonist-induced peak $[Ca^{2+}]_C$ increase, and a reduced rate of cytosolic Ca^{2+} removal following agonist stimulation. Given the unaltered capacity for ER Ca^{2+} uptake it seems unlikely that the reduced filling state of the ER Ca^{2+} store is because of changes in its physical size and/or the number and transport properties of the SERCA Ca^{2+} pumps; rather, the reduced filling state is secondary to changes in cellular ATP synthesis. Unexpectedly, we show that cytosolic ATP levels are lower in patient *versus* control cells even in the presence of high concentrations of a mitochondrial uncoupler, suggestive of extramitochondrial changes in ATP synthetic capacity. Although an exploration of the nature of these changes is beyond the scope of the present work, it is conceivable that decreases in glycolytic enzyme activity, enhanced activity of ATP-consuming mechanisms, or both are involved and represent cellular consequences of the decrease in mitochondrial oxidative capacity. Importantly, all aberrations, except for the decreased filling state of the ER, were completely restored upon acute inhibition of mitochondrial Na^+-Ca^{2+} exchange by the benzothiazepine CGP37157, presumably acting to restore agonist-induced mitochondrial ATP synthesis and thus overcoming small differences in extramitochondrial ATP synthesis or consumption.

Growing evidence suggests that under certain circumstances agonist-induced Ca^{2+} signals can turn from a survival signal into a death signal (39). For instance, agonist-induced mitochondrial Ca^{2+} uptake may induce apoptosis by activation of the permeability transition pore in response to a variety of pathological conditions (40). The cellular and molecular mechanisms underlying this switch are just beginning to be understood. Thus, enhanced formation of superoxide and hydrogen peroxide has been demonstrated to promote the Ca^{2+}-dependent opening of the permeability transition pore (41). Because the production of reactive oxygen species is increased in complex I-deficient cells (9), it is of importance to have detailed information about cytosolic and mitochondrial Ca^{2+} handling in cells with a malfunctioning complex I, especially under conditions of increased cytosolic Ca^{2+} mobilization as they occur during hormonal and electrical stimulation.

Decreased Agonist-induced Mitochondrial Ca^{2+} Uptake and Ensuing ATP Production Are Restored by CGP37157 in Complex I-deficient Fibroblasts—Under non-pathological conditions, agonist-induced mitochondrial Ca^{2+} uptake leads to an increase in mitochondrial ATP production (12, 37) through the activation of mitochondrial dehydrogenases (35). Here we show that bradykinin-induced mitochondrial Ca^{2+} uptake and ATP production are decreased in fibroblasts from a patient with isolated complex I deficiency. Importantly, CGP37157 restored the bradykinin-induced increase in both $[Ca^{2+}]_M$ and $[ATP]_M$, indicating that the reduction in mitochondrial ATP production observed in agonist-stimulated patient fibroblasts is because of a decrease in mitochondrial Ca^{2+} uptake. The reduction of the bradykinin-induced peak increase in $[Ca^{2+}]_M$ was only ~20%, whereas the decrease in bradykinin-stimulated mitochondrial ATP production was ~60%. This observation is in line with previous work showing that the agonist-induced increase in $[ATP]_M$ was already abolished when the agonist-induced peak increase in $[Ca^{2+}]_M$ was reduced by no more than 40% (37). The increase in $[ATP]_M$ started ~20 s after the onset of stimulation. This lag time is in agreement with the finding that in hepatocytes the mitochondrial [NADH] increased during the first 30 s of stimulation, after which it decreased again as a result of respiratory chain activation (36). Previous work revealed that this period of increased respiratory chain activity outlasted the return of $[Ca^{2+}]_C$ and $[Ca^{2+}]_M$ to basal levels (19, 37).

Reduced Agonist-induced Increase in $[Ca^{2+}]_C$ Is Restored by CGP37157 in Complex I Deficiency—Stimulations performed in

the absence of external Ca^{2+} revealed that bradykinin increases $[Ca^{2+}]_C$ and, as a consequence, $[Ca^{2+}]_M$ by promoting the release of Ca^{2+} from the ER in human skin fibroblasts. Here we show that the filling state of the ER is significantly reduced in patient fibroblasts. The data presented show that this reduction is not because of a decrease in physical size of the store. Neither is this reduction because of a decrease in SERCA number and/or transport properties or an increase in Ca^{2+} leakage. Our finding that the cytosolic ATP level and, as a consequence, the rate of cytosolic Ca^{2+} removal are lower in FCCP-treated patient cells as compared with FCCP-treated control cells indicates that in patient cells glycolytic activity is decreased and/or that ATP consumption is increased. In untreated patient cells, these secondary effects of complex I deficiency may contribute to a decrease in SERCA-mediated filling of the ER Ca^{2+} store. Measurements performed with JC-1, a fluorescent dye that accumulates within the mitochondrial matrix as a function of $\Delta\Psi_M$ (32), revealed that patient fibroblasts had a decreased resting $\Delta\Psi_M$. A similar observation was reached with patient fibroblasts carrying a mitochondrial $tRNA^{Leu}$ mutation of MELAS (10). Because $\Delta\Psi_M$ drives the activity of mitochondrial ATP synthase, it is likely that less ATP is produced at lower $\Delta\Psi_M$ values. This, in turn, may lead to a decreased ATP supply to the SERCAs and, consequently, a decreased filling state of the ER. The total cellular ATP content was only slightly (5%) decreased in patient fibroblasts, a result that did not reach statistical significance. This finding suggests that the lower ER Ca^{2+} content observed in resting complex I-deficient fibroblasts is because of a reduced local supply of ATP from mitochondria to neighboring SERCA pumps.

It can be hypothesized that bradykinin releases less Ca^{2+} from the ER in patient fibroblasts and therefore evokes a reduced increase in $[Ca^{2+}]_C$ and, as a consequence, $[Ca^{2+}]_M$ in these cells. However, the present study shows that in untreated patient fibroblasts the ER Ca^{2+} content and bradykinin-induced peak increase in $[Ca^{2+}]_C$ were decreased by 21 and 13%, respectively, whereas in FCCP-treated control fibroblasts these values were 11 and 23%, respectively. Importantly, this finding indicates that the decrease in $[Ca^{2+}]_C$ observed following acute FCCP treatment cannot be because of a decrease in ER Ca^{2+} content alone. It has been demonstrated that the activity of the inositol 1,4,5-trisphosphate ($InsP_3$) receptors that mediate the agonist-induced release of Ca^{2+} from the ER is regulated by ambient $[ATP]_C$ and $[Ca^{2+}]_C$ (42). Decreases in $[ATP]_C$ have been shown to activate $InsP_3$-induced Ca^{2+} release. Here we show, however, that acute FCCP treatment, despite causing a dramatic decrease in $[ATP]_C$, decreased rather than increased the bradykinin-induced increase in $[Ca^{2+}]_C$. Other studies have shown that the activity of $InsP_3$ receptors is inhibited at high ambient $[Ca^{2+}]_C$ (28, 43–45). This opens the possibility that FCCP, by abolishing mitochondrial Ca^{2+} uptake, causes a buildup of the cytosolic Ca^{2+} concentration in the mouth of the $InsP_3$-operated Ca^{2+} channels to levels that inhibit the Ca^{2+} release process, thereby reducing the total amount of Ca^{2+} that is released from the ER into the cytosol (46). It should be noted that this buildup of the cytosolic Ca^{2+} concentration during agonist stimulation is likely to be enhanced by the dramatic reduction in $[ATP]_C$ and consequent decrease in SERCA-mediated Ca^{2+} uptake into the ER.

FCCP abolishes both the $\Delta\Psi_M$ (complete loss of mitochondrial rhodamine 123 and JC-1 staining) and the bradykinin-induced increase in $[Ca^{2+}]_M$. Based on these data we hypothesize that a decrease in $\Delta\Psi_M$, as observed in complex I-deficient fibroblasts, causes a decrease in mitochondrial Ca^{2+} uptake and thus contributes to a decrease in $InsP_3$-mediated Ca^{2+} release. Also in this case, the buildup of the cytosolic Ca^{2+} concentration in the mouth of the $InsP_3$-operated Ca^{2+} channels may be enhanced by a reduced supply of ATP to the SERCAs.

The finding that inhibition of mitochondrial Na^+-Ca^{2+} exchange restores the peak increase in $[Ca^{2+}]_C$ provides us with intriguing information about the interplay between neighboring ER Ca^{2+} channels and mitochondrial Ca^{2+} uptake and extrusion sites (47). According to the above hypothesis, the restorative action of CGP37157 in patient fibroblasts can be explained in that the drug by inhibiting mitochondrial Ca^{2+} release enhances the bradykinin-induced increase in $[Ca^{2+}]_M$ and consequent increases in dehydrogenase activity, $\Delta\Psi_M$, and ATP production. It is tempting to speculate that the increase in $\Delta\Psi_M$ promotes further Ca^{2+} uptake thus preventing the buildup of inhibitory cytosolic Ca^{2+} concentrations in the mouth of the $InsP_3$-operated Ca^{2+} channels. As a consequence, more Ca^{2+} is released from the ER into the cytoplasm leading to restoration of the bradykinin-induced increase in $[Ca^{2+}]_C$. Notably, acute treatment with CGP37157 did not restore the ER Ca^{2+} content in complex I-deficient fibroblasts, whereas it restored the bradykinin-induced increases in $[Ca^{2+}]_C$ and $[Ca^{2+}]_M$ in these cells. This observation reinforces the idea that CGP37157 exerts its restorative effect by increasing $\Delta\Psi_M$. It is unlikely that CGP37157 exerts this effect through its stimulatory action on mitochondrial ATP production and consequent SERCA activation because the increases in $[ATP]_M$ and $[ATP]_C$ clearly lag behind the increase in $[Ca^{2+}]_C$. Finally, the observation that FCCP abolished the restorative effect of CGP37157 furthermore stresses the importance of $\Delta\Psi_M$ in the mechanism of action of this drug.

Decreased Cytosolic Ca^{2+} Removal following Agonist Stimulation and Its Restoration by CGP37157 in Complex I Deficiency—A significant correlation was observed between the rate of cytosolic Ca^{2+} removal and the peak increase in $[Ca^{2+}]_C$ in bradykinin-stimulated patient fibroblasts, indicating a common cause for their reduction in human complex I deficiency. Similarly to four of the eight patient cell lines studied here, the agonist-induced peak increase in $[Ca^{2+}]_C$ was not altered in a cybrid cell line of ρ^0-osteosarcoma cells and enucleated cytoplasts from a patient with the $tRNA^{Lys}$ mutation of MERRF (12). However, in the latter study no analysis of the rate of cytosolic Ca^{2+} removal was performed. Here we show that this rate was significantly decreased in all eight complex I-deficient cell lines tested. In addition we show that acute addition of CGP37157 can restore the rate of cytosolic Ca^{2+} removal in patient fibroblasts. Based on our findings, this effect of the drug is explained in that it restores mitochondrial ATP production and thus cytosolic ATP supply to the SERCAs.

As a consequence of decreased agonist-induced mitochondrial ATP production, fueling of energy-requiring processes, set in motion by the increase in $[Ca^{2+}]_C$, becomes jeopardized. One of these processes is the energy-dependent extrusion of Ca^{2+} from the cytosolic compartment. Indeed, the present study shows that this process is significantly slowed down in bradykinin-stimulated patient fibroblasts. We demonstrated recently that the rate of sarcoplasmic Ca^{2+} removal following electrical stimulation was significantly reduced in myotubes cultured from the quadriceps muscle of patients with an adult onset of exercise intolerance and exercise-induced myalgia and stiffness exhibiting a biochemically defined decrease in mitochondrial ATP production capacity (48). It is tempting to speculate that in the long term, the cumulative effect of such longer lasting $[Ca^{2+}]_C$ rises is toxic to the cell. It has been demonstrated that sustained elevations of $[Ca^{2+}]_C$ can switch on a number of mechanisms leading to necrotic as well as apoptotic cell death (49–51). The present finding that CGP37157 can

normalize the rate of cytosolic Ca^{2+} removal by restoring mitochondrial ATP synthesis in complex I-deficient patient fibroblasts may open possibilities of future therapeutic treatment. In this context, it is of importance to realize that the drug did not affect the rate of cytosolic Ca^{2+} removal in fibroblasts from a healthy subject.

Conclusions—Intriguingly, although the OXPHOS system contains a defective complex I, it was possible to enhance mitochondrial ATP synthesis by acute treatment with CGP37157. It is of note that enzymatic deficiencies in different parts of the energy-producing cascade, like the pyruvate dehydrogenase complex, complex I, and complex IV of the OXPHOS system, may all lead to Leigh disease. It is therefore tempting to assume that Leigh disease, although genetically different, has a similar underlying pathophysiological basis of which Ca^{2+} may be the common denominator.

Acknowledgments—We thank Dr. Gabriela Da SilvaXavier (University of Bristol), Dr. Takashi Tsuboi (University of Bristol), and Martijn Wilmer (Department of Pediatrics, University Medical Center Nijmegen) for technical assistance.

REFERENCES

1. Loeffen, J., Elpeleg, O., Smeitink, J., Smeets, R., Stöckler-Ipsiroglu, S., Mandel, H., Sengers, R., Trijbels, F., and van den Heuvel, L. (2001) *Ann. Neurol.* **49,** 195–201
2. Budde, S. M. S., van den Heuvel, L. P. W. J., Janssen, A. J., Smeets, R. J. P., Buskens, C. A. F., DeMeirleir, L., van Coster, R., Baethmann, M., Voit, T., Trijbels, J. M. F., and Smeitink, J. A. M. (2000) *Biochem. Biophys. Res. Commun.* **275,** 63–68
3. Van den Heuvel, L., Ruitenbeek, W., Smeets, R., Gelman-Kohan, Z., Elpeleg, O., Loeffen, J., Trijbels, F., Mariman, E., de Bruijn, D., and Smeitink, J. (1998) *Am. J. Hum. Genet.* **62,** 262–268
4. Triepels, R. H., van den Heuvel, J. P., Loeffen, J. L. C. M., Buskens, C. A. F., Smeets, R. J. P., Rubio Gozalbo, M. E., Budde, S. M. S., Mariman, E. C., Wijburg, F. A., Barth, P. G., Trijbels, J. M. F., and Smeitink, J. A. M. (1999) *Ann. Neurol.* **45,** 787–790
5. Loeffen, J., Smeitink, J., Triepels, R., Smeets, R., Schuelke, M., Sengers, R., Trijbels, F., Hamel, B., Mullaart, R., and van den Heuvel, L. (1998) *Am. J. Hum. Genet.* **63,** 1598–1608
6. Schuelke, M., Smeitink, J., Mariman, E., Loeffen, J., Plecko, B., Trijbels, F., Stöckler-Ipsiroglu, S., and van den Heuvel, L. (1999) *Nat. Genet.* **21,** 260–261
7. Smeitink, J., van den Heuvel, L., and DiMauro, S. (2001) *Nat. Rev. Genet.* **2,** 342–352
8. Robinson, B. H., Glerum, D. M., Chow, W., Petrova-Benedict, R., Lightowlers, R., and Capaldi, R. (1990) *Pediatr. Res.* **28,** 549–555
9. Pitkänen, S., and Robinson, B. H. (1996) *J. Clin. Investig.* **98,** 345–351
10. Moudy, A. M., Handran, S. D., Goldberg, M. P., Ruffin, N., Karl, I., Kranz-Eble, P., DeVivo, D. C., and Rothman, S. M. (1995) *Proc. Natl. Acad. Sci. U. S. A.* **92,** 729–733
11. Vazquez-Memije, M. E., Shanske, S., Santorelli, F. M., Kranz-Eble, P., Davidson, E., DeVivo, D. C., and DiMauro, S. (1996) *J. Inherit. Metab. Dis.* **19,** 43–50
12. Brini, M., Pinton, P., King, M. P., Davidson, M., Schon, E. A., and Rizzuto, R. (1999) *Nat. Med.* **5,** 951–954
13. Carrozzo, R., Tessa, A., Vázquez-memije, M. E., Piemonte, F., Patrono, C., Malandrini, A., Dionisi-Vici, C., Vilarinho, L., Villanova, M., Schägger, H., Federico, A., Bertini, E., and Santorelli, F. M. (2001) *Neurology* **56,** 687–690
14. Van der Westhuizen, F. H., van den Heuvel, L. P., Smeets, R., Veltman, J. A., Pfundt, R., van Kessel, A. G., Ursing, B. M., and Smeitink, J. A. M. (2003) *Neuropediatrics* **34,** 14–22
15. Ahlers, P. M., Garofano, A., Kerscher, S. J., and Brandt, U. (2000) *Biochim. Biophys. Acta* **1459,** 258–265
16. Weidner, U., Geier, S., Ptock, A., Friedrich, T., and Weiss, H. (1993) *J. Mol. Biol.* **233,** 109–122
17. Ahlers, P. M., Zwicker, K., Kerscher, S., and Brandt, U. (2000) *J. Biol. Chem.* **275,** 23577–23582
18. Koopman, W. J. H., Bosch, R. R., van Emst-de Vries, S. E., Spaargaren, M., De Pont, J. J. H. H. M., and Willems, P. H. G. M. (2003) *J. Biol. Chem.* **278,** 13672–13679
19. Ainscow, E. K., and Rutter, G. A. (2001) *Biochem. J.* **353,** 175–180
20. Ainscow, E. K., and Rutter, G. A. (2002) *Diabetes* **51,** S162–S170
21. Montero, M., Brini, M., Marsault, R., Alvarez, J., Sitia, R., Pozzan, T., and Rizzuto, R. (1995) *EMBO J.* **14,** 5467–5475
22. Rutter, G. A., Theler, J. M., Murgia, M., Wollheim, C. B., Pozzan, T., and Rizzuto, R. (1993) *J. Biol. Chem.* **268,** 22385–22390
23. Brini, M., Marsault, R., Bastianutto, C., Alvarez, J., Pozzan, T., and Rizzuto, R. (1995) *J. Biol. Chem.* **270,** 9896–9903
24. van de Put, F. H., De Pont, J. J. H. H. M., and Willems, P. H. G. M. (1994) *J. Biol. Chem.* **269,** 12438–12443
25. Alvarez, J., and Montero, M. (2002) *Cell Calcium* **32,** 251–260
26. Assimacopolous-Jeannet, F., McCormack, J. G., and Jeanrenaud, B. (1986) *J. Biol. Chem.* **261,** 8799–8804
27. Rizzuto, R., Simpson, A. W. M., Brini, M., and Pozzan, T. (1992) *Nature* **358,** 325–327
28. Rizzuto, R., Brini, M., Murgia, M., and Pozzan, T. (1993) *Science* **262,** 744–747
29. Gunter, K. K., and Gunter, T. E. (1994) *J. Bioenerg. Biomembr.* **26,** 471–485
30. Bernardi, P. (1999) *Physiol. Rev.* **79,** 1127–1155
31. Kirichok, Y., Krapivinsky, G., and Clapham, D. E. (2004) *Nature* **427,** 360–364
32. Smiley, S. T., Reers, M., Mottola-Hartshorn, C., Lin, M., Chen, A., Smith, T. W., Steele, G. D., and Chen, L. B. (1991) *Proc. Natl. Acad. Sci. U. S. A.* **88,** 3671–3675
33. Denton, R. M., and McCormack, J. G. (1990) *Annu. Rev. Physiol.* **52,** 451–466
34. Rutter, G. A. (1990) *Int. J. Biochem.* **22,** 1081–1088
35. Hajnóczky, G., Robb-Gaspers, L. D., Seitz, M. B., and Thomas, A. P. (1995) *Cell* **85,** 415–424
36. Robb-Gaspers, L. D., Burnett, P., Rutter, G. A., Denton, R. M., Rizzuto, R., and Thomas, A. P. (1998) *EMBO J.* **17,** 4987–5000
37. Jouaville, L. S., Pinton, P., Bastianutto, C., Rutter, G. A., and Rizzuto, R. (1999) *Proc. Natl. Acad. Sci. U. S. A.* **96,** 13807–13812
38. Cox, D. A., and Matlib, M. A. (1993) *J. Biol. Chem.* **268,** 938–947
39. Orrenius, S., Zhivotovsky, B., and Nicotera, P. (2003) *Nat. Rev. Mol. Cell Biol.* **4,** 552–565
40. Hajnoczky, G., Davies, E., and Madesh, M. (2003) *Biochem. Biophys. Res. Commun.* **304,** 445–454
41. Madesh, M., and Hajnoczky, G. (2001) *J. Cell Biol.* **155,** 1003–1015
42. Patel, S., Joseph, S. K., and Thomas, A. P. (1999) *Cell Calcium* **25,** 247–264
43. Rizzuto, R., Bastianutto, C., Brini, M., Murgia, M., and Pozzan, T. (1994) *J. Cell Biol.* **126,** 1183–1194
44. Rapizzi, E., Pinton, P., Szabadkai, G., Wieckowski, M. R., Vandecasteele, G., Baird, G., Tuft, R. A., and Fogarty, K. E. (2002) *J. Cell Biol.* **159,** 613–624
45. Szabadkai, G., Simoni, A. M., and Rizzuto, R. (2003) *J. Biol. Chem.* **278,** 15153–15161
46. Bezprozvanny, I., Watras, J., and Ehrlich, B. E. (1991) *Nature* **351,** 751–754
47. Csordas, G., Thomas, A. P., and Hajnoczky, G. (1999) *EMBO J.* **18,** 96–108
48. Koopman, W. J. H., Renders, M., Oosterhof, A., van Kuppevelt, T. M., van Engelen, B. G., and Willems, P. H. G. M. (2003) *Am. J. Physiol. Cell Physiol.* **285,** C1263–C1269
49. Khan, A. A., Soloski, M. J., Sharp, A. H., Schilling, G., Sabatini, D. M., Li, S. H., Ross, C. A., and Snyder, S. H. (1996) *Science* **273,** 503–507
50. Nicotera, P., and Orrenius, S. (1998) *Cell Calcium* **23,** 173–180
51. Wang, H. G., Pathan, N., Ethell, I. M., Krajewski, S., Yamaguchi, Y., Shibasaki, F., McKeon, F., Bobo, T., Franke, T. F., and Reed, J. C. (1999) *Science* **284,** 339–343